Environmental Science & Technology

Article

Cite This: Environ. Sci. Technol. 2019, 53, 1334−1343

pubs.acs.org/est

Bulk pH and Carbon Source Are Key Factors for Calcium Phosphate Granulation

Jorge Ricardo Cunha,[†] Sara Morais,[§] Joana C. Silva,[§] Renata D. van der Weijden,*[,†,‡] Lucía Hernández Leal,[†] Grietje Zeeman,[‡] and Cees J. N. Buisman[†,‡]

[†]Wetsus, European Centre of Excellence for Sustainable Water Technology, Post Office Box 1113, 8900 CC Leeuwarden, Netherlands

[‡]Sub-department of Environmental Technology, Wageningen University, Post Office Box 17, 6700 AA Wageningen, Netherlands

[§]Department of Chemical Engineering, Faculty of Engineering of the University of Porto (FEUP), Rua Dr. Roberto Frias, 4200-465 Porto, Portugal

Supporting Information

ABSTRACT: Recovery of calcium phosphate granules (CaP granules) from high-strength wastewater is an opportunity to reduce the natural phosphorus (P) scarcity, geographic imbalances of P reserves, and eutrophication. Formation of CaP granules was previously observed in an upflow anaerobic sludge bed (UASB) reactor treating source separated black water and is enhanced by Ca^{2+} addition. However, the required operating conditions and influent composition for CaP granulation are still unknown. In this study, we have experimentally demonstrated that the carbon source and bulk pH are crucial parameters for the formation and growth of CaP granules in a UASB reactor, operating at relatively low upflow velocity (<1 cm h^{-1}). Degradation of glucose yielded sufficient biomass (microbial cells and extracellular biopolymers) to cover crystal and amorphous calcium phosphate [$Ca_x(PO_4)_y$], forming CaP granules. Influent only containing volatile fatty acids as the carbon source did not generate CaP granules. Moreover, bulk pH between 7.0 and 7.5 was crucial for the enrichment of $Ca_x(PO_4)_y$ in the granules over bulk precipitation. Bulk pH 8 reduced the $Ca_x(PO_4)_y$ enrichment in granules of >1.4 mm diameter from 9 to 5 wt % P. Moreover, for bulk pH 7.5, co-precipitation of $CaCO_3$ with $Ca_x(PO_4)_y$ was reduced.

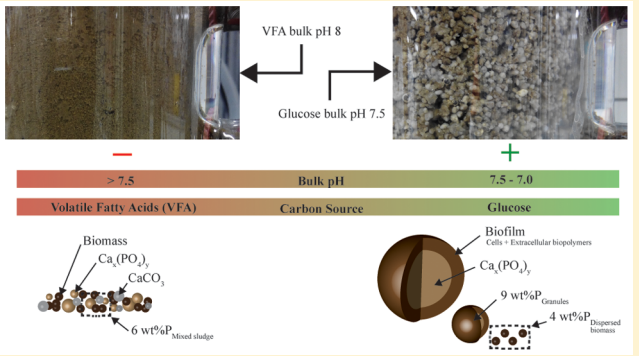

1. INTRODUCTION

Recovery of calcium phosphate granules (CaP granules) in anaerobic treatment of high-strength wastewater is a potential opportunity to decrease the human footprint on the natural phosphorus (P) cycle by reducing the impact of phosphate rock scarcity and geographic imbalances on the global food security and preventing eutrophication from P discharge in natural water courses.

The formation of CaP granules was first observed by Tervahauta et al. in an upflow anaerobic sludge bed (UASB) reactor treating vacuum-collected black water (BW).[1] Without the addition of chemicals, 2−8% of total P in BW was found as CaP granules.[2,3] With the addition of Ca^{2+}, the percentage of P harvested as CaP granules from the total P fed increased to 31%, but 89% of the total P fed accumulated in the sludge bed of the UASB reactor. Precipitation of calcium phosphate species [$Ca_x(PO_4)_y$] within existing granules over bulk precipitation is favored by a local microenvironment with an increasing pH gradient from 7.5 at the edge to 8 in the granule center.[4] Moreover, Batstone et al., who modeled substrate degradation kinetics in anaerobic granular sludge using the anaerobic digestion model number 1 (ADM1), observed that, generally, the pH increased from the edge to the granule center.[5] Conversion of organic acids into CH_4 and CO_2 (acetoclastic methanogenesis) and CO_2 plus H_2 into CH_4 (hydrogenotrophic methanogenesis) in the granule caused the pH gradient.[4,5] However, the internal pH varied with type and concentration of organic substrates in bulk liquid (wastewater).[5] Therefore, in this study, the effect of bulk pH and substrate type on CaP granulation is separately investigated to reveal the required conditions for formation and growth of CaP granules.

In vacuum-collected BW, approximately 30% of the total chemical oxygen demand (COD) is soluble, of which 50−70% are volatile fatty acids (VFA) rapidly degraded at the bottom of the reactor, according to Graaff et al. and Cunha et al.[3,6] Although the collection can greatly influence the composition

Received: November 5, 2018
Revised: December 27, 2018
Accepted: January 8, 2019
Published: January 8, 2019

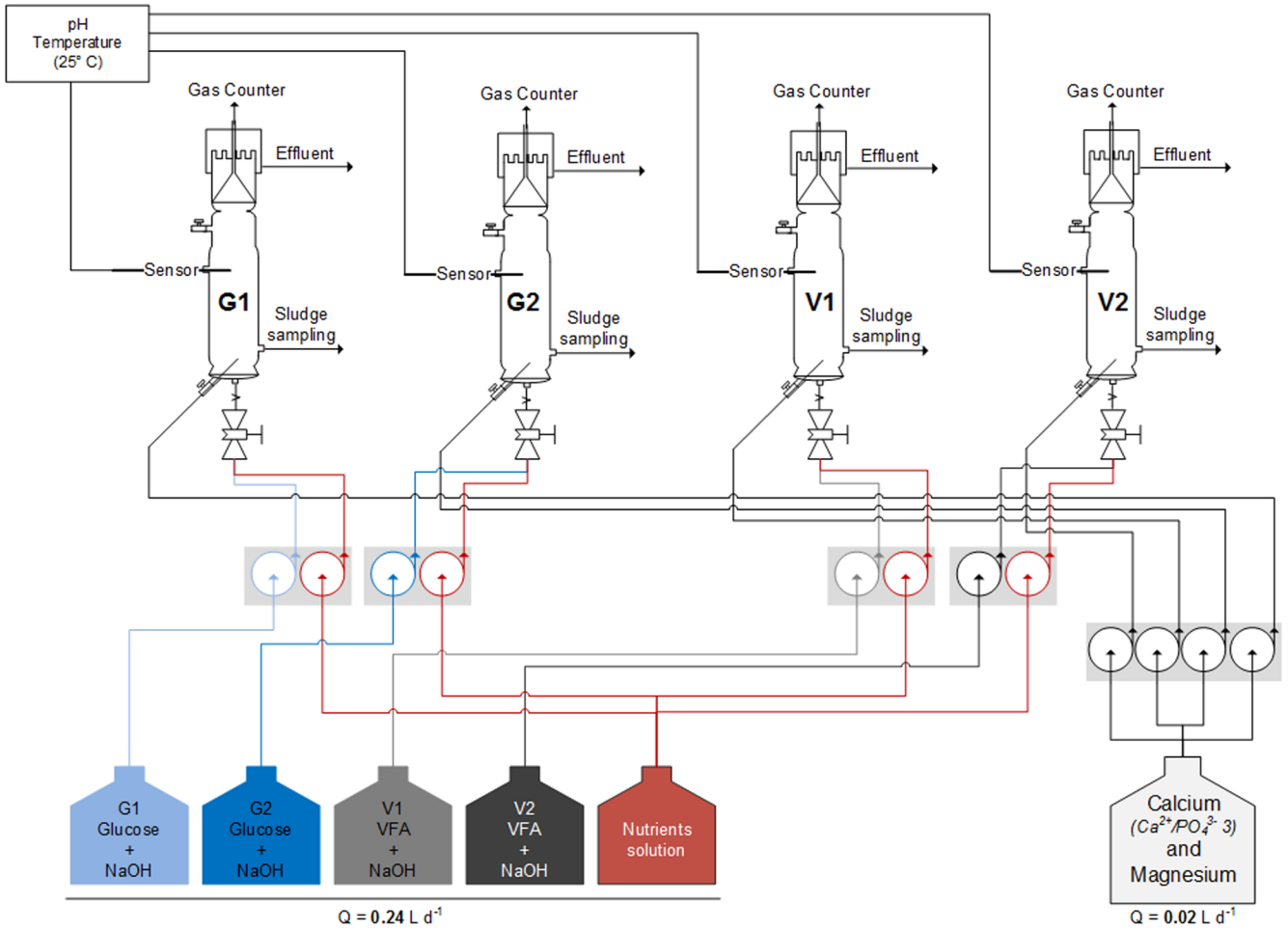

Figure 1. Schematic representation of the experimental setup.

of BW, the largest fraction of the total COD is in the solid phase. Thus, it is generally accepted that hydrolysis of solids is the rate-limiting step (k_h of 0.1 day^{-1}) for anaerobic treatment of BW.[3,6,7] Consequently, acidogenesis, acetogenesis, and methanogenesis are kinetically dependent upon the hydrolysis.[8] Liu et al. reported that substrate limitation (stress) is one of the major causes for granulation by stimulating the production of extracellular biopolymers or extracellular polymeric substances (EPS).[9] The agglomeration of biopolymers and microorganisms creates a structural matrix where microbial syntrophy (exchange of byproducts) is kinetically favored.[10] Schmidt and Ahring, who determined the concentration and composition of biopolymers in granular sludge, measured lower concentrations of polysaccharides and proteins in the biopolymer matrix in granular sludge fed with VFA when compared to granular sludge fed with wastewater from the sugar factory, paper mill, and fish meal process.[11] This is an indication that the yield of biopolymers is enhanced when hydrolysis and/or acidogenesis are required process steps during the substrate conversion to CH_4. Thus, during anaerobic treatment of BW, formed biopolymers are likely stimulating the formation of CaP granules by enhancing agglomeration of organic and $Ca_x(PO_4)_y$ particles, which is the foundation for CaP granulation.[4] The addition of extra Ca^{2+} (250 mg L^{-1}) increased the production of CaP granules by directly increasing the formation and growth of $Ca_x(PO_4)_y$ particles.[3] Additionally, the formation of bridges between Ca^{2+} and negatively charged biopolymers and microbial cells may have stimulated the formation of CaP granules by strengthening the organic matrix and, consequently, the capture and agglomeration of $Ca_x(PO_4)_y$ particles.[12]

The effect of bulk pH, substrate degradation [high and low energy of reaction ($\Delta G°$)], and production of biopolymers on CaP granulation was investigated by monitoring four lab-scale UASB reactors. Two bioreactors were fed with glucose at bulk pH 7.5 and 8 to stimulate biopolymer production. The other two bioreactors were fed with a VFA mixture at bulk pH 7.5 and 8 to limit biopolymer production. A simulated BW matrix (anions and cations) was fed to all bioreactors. Then, treatment performance was determined by measuring COD and PO_4^{3-} removals and CH_4 production. CaP granulation was assessed by particle size, elemental (P, Ca, and Mg), and X-ray diffraction (XRD) analyses.

2. EXPERIMENTAL SECTION

2.1. Experimental Setup and Influent Composition. Four 2 L lab-scale UASB reactors (G1, G2, V1, and V2) were operated at 25 °C with an aimed hydraulic retention time (HRT) of 4 days and organic loading rate (OLR) of 1 g of COD L^{-1} day^{-1} (Figure 1). The inoculum (1 L for each reactor) was obtained from a full-scale UASB reactor treating BW[13] and sieved before inoculation to remove particles of >0.4 mm diameter. Applied substrates were glucose for G1 and G2 and VFA mixture (60, 20, and 20% of acetate, propionate, and

DOI: 10.1021/acs.est.8b06230
Environ. Sci. Technol. 2019, 53, 1334−1343

Table 1. Key Parameters of Operational Conditions and Treatment Performance for Each Reactor between Operation Days 100 and 200

		G1		G2		V1		V2	
	unit	glucose	sd	glucose	sd	VFA	sd	VFA	sd
bulk pH		7.49	0.10	8.06	0.39	7.72	0.08	8.20	0.16
organic loading rate (OLR)	g of COD L^{-1} day^{-1}	1.0	0.1	1.0	0.1	0.8	0.1	0.9	0.1
total COD influent	g of COD L^{-1}	3.9	0.1	3.7	0.4	3.4	0.3	3.4	0.3
hydraulic retention time (HRT)	days	3.9	0.5	4.1	1.0	4.1	0.7	3.8	0.4
total COD removal	%	88	2	76	9	95	6	73	14
VFA removal	%					93	8	65	19
VFA effluent	g of COD L^{-1}	0.04	0.02	0.25	0.19	0.06	0.04	0.53	0.25
solid COD effluent	g of COD L^{-1}	0.07	0.05	0.33	0.3	0.05	0.06	0.15	0.08
methanization	g of COD CH_4 g^{-1} of COD influent	0.7	0.1	0.4	0.2	0.9	0.1	0.5	0.1
sludge production (measured)[a]	g of COD-VSS g^{-1} of COD influent	0.11		0.08		0.04		0.05	
sludge production (calculated)[b]	g of COD g^{-1} of COD influent	0.18		0.36		0.05		0.23	
COD missing	%	7		28		1		18	
PO_4^{3-} influent loading	mg day^{-1}	104	29	101	36	100	29	111	37
Ca^{2+} influent loading	mg day^{-1}	119	10	112	18	113	10	120	16
influent $n[Ca^{2+}]/n[PO_4^{3-}]$	mol/mol	2.7	1.0	2.6	1.4	2.7	1.0	2.6	1.2
PO_4^{3-} removal	%	88	2	91	5	90	3	85	5
Ca^{2+} removal	%	45	11	77	10	64	7	82	5
inorganic carbon effluent	mg of C L^{-1}	545	50	602	83	620	46	572	97
HCO_3^- effluent	g L^{-1}	2.58	0.24	2.99	0.41	3.01	0.22	2.84	0.48

[a]Considering the VSS concentration at the bottom (sampling location) and the sludge bed height. [b]Accumulated COD based on COD influent minus COD effluent and COD CH_4.

butyrate on a COD basis, respectively) for V1 and V2. Nutrients were mixed with the substrates just before the reactor inlet. Ca^{2+} and Mg^{2+} were separately fed to each reactor to avoid precipitation in the inlet system. The flow of the substrate, nutrients, and Ca^{2+} and Mg^{2+} solutions was 0.24 L day^{-1} (48%), 0.24 L day^{-1} (48%), and 0.02 L day^{-1} (4%), respectively. The substrate solution for G1 and G2 contained 7.8 g L^{-1} of $C_6H_{12}O_6$ (glucose), and the substrate solution for V1 and V2 contained 6.4 g L^{-1} of $C_2H_3NaO_2$, 1.1 mL L^{-1} of $C_3H_6O_2$, and 0.9 mL L^{-1} of $C_4H_8O_2$. The nutrient solution, which was prepared according to the soluble chemical composition of BW,[6] was equal for all reactors and contained 2.3 g L^{-1} $KHCO_3$, 1.5 g L^{-1} $Na_3PO_4{\cdot}12H_2O$, 8.6 g L^{-1} NH_4Cl, 3.8 g L^{-1} $NaHCO_3$, and 0.2 g L^{-1} $(NH_4)_2SO_4$. Additionally, trace elements were added according to Angelidaki et al.[14] The Ca^{2+} and Mg^{2+} solution contained 21.4 g L^{-1} $CaCl_2{\cdot}2H_2O$ and 0.8 g L^{-1} $MgCl_2{\cdot}6H_2O$. Ca^{2+} was added to obtain a Ca^{2+}/PO_4^{3-} molar ratio of 3, which is sufficient for P removal as previously observed by Seckler et al.[15] The chemical composition of each solution was experimentally determined. Nutrients and Ca^{2+} and Mg^{2+} solutions were assessed for pH, elements (P, Ca, Mg, Na, K, and S), anions (PO_4^{3-}, Cl^-, and SO_4^{2-}), cations (NH_4^+, Ca^{2+}, and Mg^{2+}), total organic carbon (TOC), and inorganic carbon (IC). The latter was combined with pH, which was measured right after sampling, using a precalibrated Endress+Hauser sensor, to calculate the HCO_3^- concentration according to eq 1

$$[HCO_3^-] = \frac{IC(10^{-pH})k_{a1}}{((10^{-pH}))^2 + (10^{-pH})k_{a1} + k_{a1}k_{a2}} \quad (1)$$

where $k_{a1} = 4.467 \times 10^{-7}$ mol L^{-1} and $k_{a2} = 4.477 \times 10^{-11}$ mol L^{-1} (25 °C).[8]

Substrate solutions were assessed for total and soluble COD, VFA (acetate, propionate, and butyrate), and total organic carbon (TOC). The effluent of each reactor was assessed weekly for soluble and total elements, anions, cations, TOC, inorganic carbon (IC), total and soluble COD, and VFA. The bulk pH for each reactor was measured on top of each reactor using Endress+Hauser sensors precalibrated with pH 7 and 9 buffer solutions (VWR Chemicals, Netherlands). The bulk pH was controlled manually by dosing NaOH in each substrate solution.

2.2. Physical and Chemical Analyses. Concentration of elements was measured with inductively coupled plasma optical emission spectrometry (ICP−OES, PerkinElmer Optima 5300 DV). For soluble elements, samples were prefiltered with 0.45 μm membrane Cronus filter polytetrafluoroethylene (PTFE). For total elements, unfiltered samples were digested with HNO_3 in combination with microwave-induced heating (MWD Milestone) at 148 °C during 45 min prior to ICP−OES analysis. Concentrations of anions, cations, and VFA were measured with ion chromatography (Metrohm 761 Compact) using membrane-filtered samples. TOC and IC concentrations were measured with a Shimadzu TOC analyzer after membrane filtration. COD was measured with cuvette tests Hach Lange (LCK114).

2.3. Particle Size Distribution Analysis. Sludge (60 mL) was sampled at 5 cm from the bottom of each reactor on days 56, 89, 126, 152, 195, and 217 of operation. Then, particle size distribution was measured through a sequential separation using mesh sieves with mesh sizes of 1.4, 0.9, and 0.4 mm. Collected particle fractions had >1.4, 1.4−0.9, 0.9−0.4, and <0.4 mm diameters. The total suspended solids (TSS) and volatile suspended solids (VSS) concentrations and elemental composition were determined for each size fraction (except samples of day 152). TSS and VSS were assessed with the standard gravimetric method,[16] and elemental composition was measured using ICP−OES on solid samples after drying at 105 °C for at least 12 h and digested with HNO_3, as aforementioned. Particle fractions from day 56 were also assessed with XRD, using a Bruker D8 Advance diffractometer

DOI: 10.1021/acs.est.8b06230
Environ. Sci. Technol. 2019, 53, 1334−1343

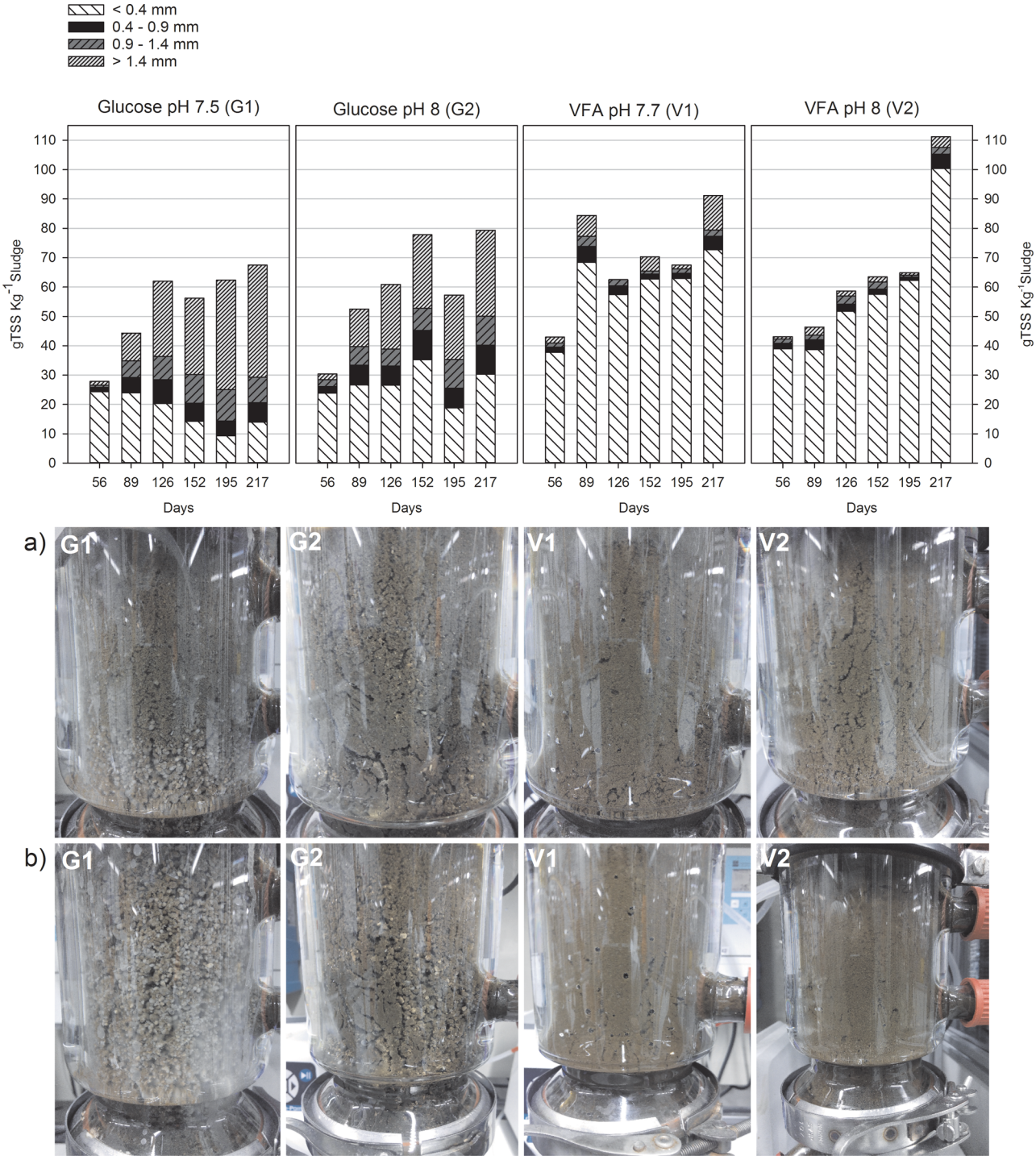

Figure 2. (Top) Particle size distribution (<0.4, 0.4−0.9, 0.9−1.4, and >1.4 mm diameter) of the sludge bed at 5 cm from the bottom of each reactor. Photos of the sludge bed for each reactor on operation days (a) 102 and (b) 126.

with Cu radiation. The samples were dried at 105 °C for 12 h and ground before the measurements. Granule samples (>1.4 mm diameter), which were taken from G1 after the operation period (217 days), were subjected to a prefixation step using glutaraldehyde (2.5%) as described by Ismail et al.[17] Then, they were visualized with a scanning electron microscope (JEOL JSM-6480LV) for structural analysis.

2.4. Extraction and Quantification of Biopolymers. Extraction of soluble, loose, and bound biopolymers was performed through a sequential extraction using a cation-exchange resin (CER) as described by Frolund et al. for each reactor.[18] Loose and bound biopolymers were quantified for all particle size fractions of reactors G1 and G2 and only for particles of <0.4 mm diameter for V1 and V2. Soluble biopolymers or bulk biopolymers were measured in the supernatant after separation of particles of <0.4 mm diameter. Each size fraction was resuspended in 100 mM NaCl solution and stirred at 1000 rpm for 3 h to extract the loose fraction of biopolymers. After centrifugation (12000*g* for 10 min), the loose biopolymers were then quantified in the supernatant.

DOI: 10.1021/acs.est.8b06230
Environ. Sci. Technol. 2019, 53, 1334−1343

The pellet was resuspended once more with the NaCl solution and mixed with pre-washed CER at a concentration of 70 g g^{-1} of VSS. CER was washed with 1× phosphate-buffered saline (PBS) buffer solution for 1 h while stirring at 300 rpm. The mixture of resuspended pellet and CER was stirred for 2 h at 600 rpm and 4 °C to extract the bound fraction of biopolymers and subsequently centrifuged (12000*g* for 15 min). The bound biopolymers were then measured in the supernatant.

The quantification of biopolymers was determined in a carbon basis by liquid chromatography−organic carbon detection (LC−OCD, model 8 with a NDIR detector Siemens Ultramat 6^E and UV and OND detector Agilent 1260 Infinity) after a 0.22 μm membrane filtration (Thermo Scientific Nalgene filter) to remove microbial cells and debris. Because of the high Ca^{2+} concentration, the biopolymer quantification could be significantly underestimated by the formation of complexes, which are removed from the liquid by the 0.22 μm filtration step. Thus, the TOC concentration was determined without the filtration step to evaluate the effect of Ca^{2+}. Then, colloidal carbon is estimated by subtracting dissolved organic carbon (DOC) obtained by LC−OCD from TOC.

3. RESULTS AND DISCUSSION

3.1. Treatment Performance and Operational Conditions. Stabilization of bulk pH and methanization was reached after 100 days of operation for all reactors (Figure S2.1 and Table S2.1 of the Supporting Information). Thus, the steady state is assumed between operation days 100 and 200. In Table 1, the bulk pH and the key performance parameters for the treatment efficiency of each reactor are then presented for the steady-state period. The effect of the carbon source and bulk pH on the calcium phosphate granulation are separately presented and discussed in the following subsections.

With regard to COD removal, the increase in bulk pH for G2 and V2 resulted in a reduction in the overall COD removal and methanization rate when compared to G1 and V1. This can be explained by pH inhibition on the degradation of glucose and VFA.[19−23] In G2 and V2, a higher percentage of COD was missing in the mass balance (28 and 18%, respectively) compared to G1 and V1 (7 and 1%, respectively). A foam layer above the gas−liquid−solid separator was observed for G2 and V2, which likely contributed to the COD removal but not the methanization. The relatively high concentration of VFA leaving the reactors G2 and V2 could have acted as a surfactant, inducing the foam formation.[24] According to the COD balance, the estimated concentration of COD trapped on top of G2 and V2 was 1.1 and 0.6 g of COD L^{-1}, respectively. For V1, the pH stabilized at 7.7 ± 0.1, although NaOH dosing (6 mM) stopped after 140 days of operation.

For PO_4^{3-} removal, the increase in bulk pH for G2 (pH 8.1) and V2 (pH 8.2) did not significantly affect the PO_4^{3-} removal efficiency when compared to G1 and V1 (Table 1). Thus, bulk pH 7.5 (G1) is sufficient to decrease the PO_4^{3-} concentration from 64 ± 15 mg of P L^{-1} in the influent to 7.6 ± 1.4 mg of P L^{-1} in the effluent (88% removal), when Ca^{2+} was added at Ca^{2+}/PO_4^{3-} molar ratio of 2.7. At bulk pH 7, the PO_4^{3-} removal for both G1 and G2 decreased to 70% and decreased further for bulk pH lower than 7.0 (left panel of Figure S2.2 of the Supporting Information). This is explained by a reduction in the ionic activity of HPO_4^{2-} and an increase of $H_2PO_4^-$ (pK_a = 7.21), diminishing $Ca_x(PO_4)_y$ formation.[25]

Removal of Ca^{2+} was proportional to bulk pH (Table 1 and Figure S2.2 of the Supporting Information), indicating that Ca^{2+} removal was not influenced by the substrate use but rather dependent upon the bulk pH. For G1, the Ca^{2+}/PO_4^{3-} molar ratio of accumulated and/or precipitated Ca^{2+} and PO_4^{3-} was 1.6 ± 0.9, while for G2, V1, and V2, the Ca^{2+}/PO_4^{3-} molar ratio was 2.56 ± 1.34, 2.17 ± 1.02, and 2.97 ± 1.38, respectively. The Ca^{2+}/PO_4^{3-} molar ratio obtained for G1 was close to the theoretical Ca^{2+}/PO_4^{3-} molar ratio of hydroxyapatite (1.67). For G2, V1, and V2, the Ca^{2+}/PO_4^{3-} molar ratio was greater than the reference value for hydroxyapatite, indicating that part of accumulated Ca^{2+} was used for other purposes than $Ca_x(PO_4)_y$ formation. For V1 (bulk pH 7.7), the higher HCO_3^- concentration when compared to G1 (Table 1) induced a higher co-precipitation of $CaCO_3$, although the bulk pH was lower than in V2; the higher HCO_3^- concentration in V1 originated from the higher degree of neutralized VFA degradation in the reactor.

3.2. Role of the Carbon Source in CaP Granulation. Granule formation was observed for both reactors fed with glucose (G1 and G2) after 89 days of operation (Figure 2). The concentration of particles of >0.4 mm diameter between operation days 126 and 217 was 47 ± 5 and 42 ± 4 g of TSS L^{-1}_{sludge} for G1 and G2, respectively, representing 79 ± 7 and 62 ± 6% of the total TSS concentration. The lower percentage of granules in G2 compared to G1 can be explained by the higher level of Ca^{2+} precipitation in the bulk, which led to the formation of fine particles (<0.4 mm diameter), decreasing the percentage of particles of >0.4 mm diameter. Note that the average concentration of particles of >0.4 mm diameter in G1 and G2 for the same period was similar. For the reactors fed with the VFA mixture (V1 and V2), granule formation was nearly absent; the percentage of particles of >0.4 mm diameter between operation days 126 and 217 was 12 ± 7% (10 ± 8 g of TSS L^{-1}_{sludge}) and 8 ± 4% (7 ± 4 g of TSS L^{-1}_{sludge}) for V1 and V2, respectively. Thus, the bulk pH had a trivial effect on the granule formation when compared to the substrate type. The sharp increase in the concentration of particles of <0.4 mm diameter in V2 from days 195 to 217 (Figure 2) is likely due to an increase in the amount of calcium precipitates in between the biomass at the sampling location (5 cm from the bottom of the reactor). This is in line with the lower concentration of VSS (28 wt %) in particles of <0.4 mm diameter from V2 on day 217 when compared to the global average of VSS content for V2 (35 wt %), as shown further in Figure 4.

The previous study from Cunha et al. proposed that CaP granulation occurs through agglomeration of biomass and inorganic precipitates and is enhanced by the addition of the divalent cation Ca^{2+}, which contributes to the agglomeration by bridging with negatively charged biomass (microorganisms and extracellular biopolymers).[3] The higher free energy available during anaerobic degradation of glucose (ΔG°_{STP} of −212 kJ mol^{-1}) compared to the VFA mixture was likely the key factor behind the formation of granules in G1 and G2.[8,21,26] Note that ΔG°_{STP} for acetate is −31 kJ mol^{-1}, but ΔG°_{STP} for butyrate and propionate is +48 and +76 kJ mol^{-1}, respectively, requiring a H_2 partial pressure between 10^{-4} and 10^{-6} atm for generating energy (ΔG° from 0 to −25 kJ mol^{-1}), which is reached under anaerobic conditions.[27] The higher ΔG° of glucose resulted in a higher VSS yield (biomass and extracellular biopolymers) compared to the VFA mixture as the substrate.[8] Consequently, the amount of organic material available for granule formation and growth increased. The

DOI: 10.1021/acs.est.8b06230
Environ. Sci. Technol. 2019, 53, 1334−1343

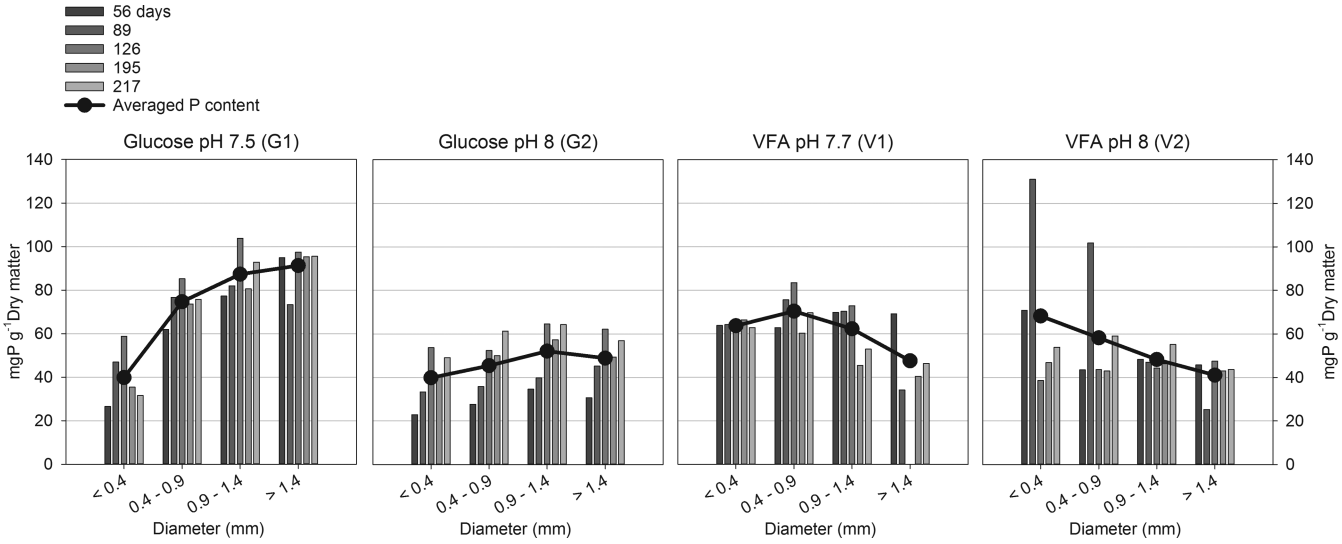

Figure 3. P content in dry matter from each size fraction over time and the average for each size fraction for each reactor.

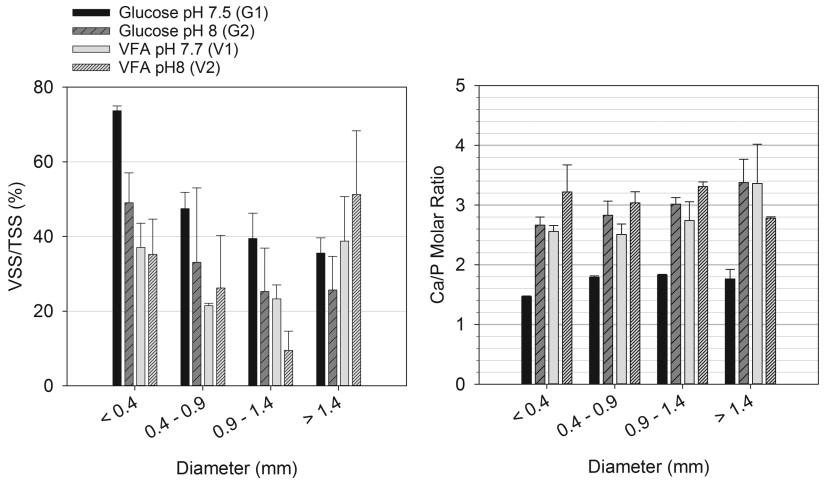

Figure 4. (Left) Average percentage of VSS in TSS and (right) Ca/P molar ratio in dry solids from each size fraction for each reactor. (Right) Average percentages were obtained from measurements on operation days 195 and 217.

concentration of soluble and bound biopolymers for each particle size from each reactor is shown in Figure S3.1 of the Supporting Information. The concentration of bound biopolymers in particles of <0.4 mm diameter from G1 (13.2 ± 0.1 mg of C g^{-1} of VSS) and G2 (9.1 ± 0.1 mg of C g^{-1} of VSS) was 2.4 and 1.7 times and 2.7 and 1.8 times higher than in particles from V1 (5.5 ± 0.2 mg of C g^{-1} of VSS) and V2 (4.9 ± 0.1 mg of C g^{-1} of VSS), respectively. For loose biopolymers, the result was similar (Figure S3.1 of the Supporting Information). Liu et al. demonstrated that both fractions, loose and bound biopolymers, have a substantial contribution toward biomass aggregation.[28] Moreover, Ding et al., who reviewed the role of extracellular biopolymers in bioaggregation, showed that production of biopolymers is one of the major biological forces ensuring stability and granule maturation.[29] The hypothesized contribution of extracellular biopolymers to CaP granulation consists of two factors: (1) physical entrapment of $Ca_x(PO_4)_y$ particles and microorganisms by the extracellular biopolymers and subsequent growth of the $Ca_x(PO_4)_y$ core along with the internal biomass decay and (2) internal higher supersaturation for $Ca_x(PO_4)_y$ (or higher Ca^{2+} ionic activity) enhanced by binding of Ca^{2+} with negatively charged biopolymers.

Common anaerobic granulation is stimulated by applying an upflow velocity in the UASB reactor of >100 cm h^{-1}.[30−32] However, the upflow velocity applied in all reactors (G1, G2, V1, and V2) of this study was <1 cm h^{-1} to simulate the conditions during anaerobic treatment of real BW.[3] Thus, the formation of granules in this study did not depend upon the upflow velocity as in common anaerobic biomass but rather the production of extracellular biopolymers using glucose as the substrate compared to the VFA mixture. The produced biopolymers stimulated the formation of the biofilm surrounding the $Ca_x(PO_4)_y$ core as previously observed.[1,3] Then, syntrophic metabolism between H_2 producers and consumers (acetogens and methanogens) within the biopolymer matrix induced the pH gradient, which favored enrichment of $Ca_x(PO_4)_y$ in the granules over bulk precipitation. Thus, insufficient organic material to form the outer biofilm and, consequently, the absence of concentrated acetoclastic and hydrogenotrophic methanogenesis to induce the pH gradient restrict CaP granulation, as shown in V1.

DOI: 10.1021/acs.est.8b06230
Environ. Sci. Technol. 2019, 53, 1334−1343

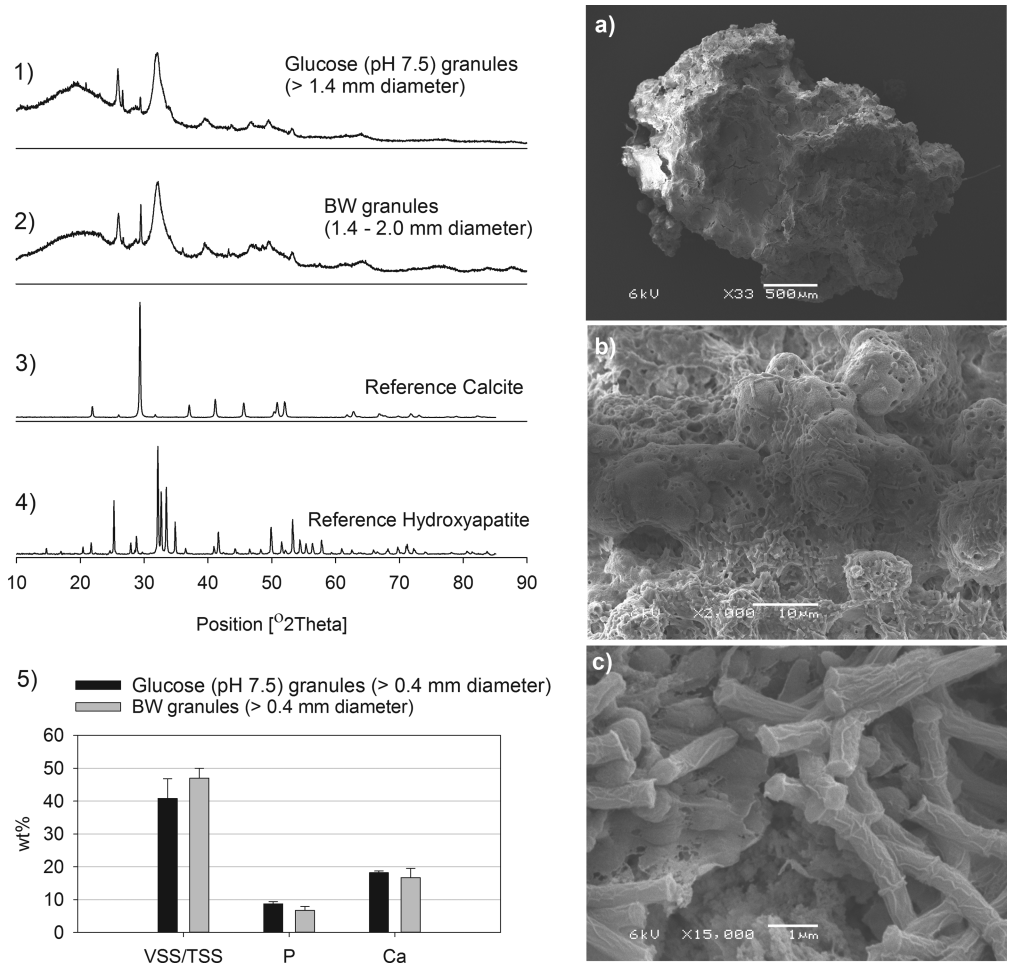

Figure 5. XRD patterns of glucose granules (>1.4 mm diameter) from (1) G1 and (2) BW granules and (3 and 4) reference patterns of calcite and hydroxyapatite, respectively. (5) Elemental composition of glucose (pH 7.5) and BW granules. Scanning electron microscope images of (a) representative glucose granule from G1 and magnified images of the (b) granule surface and (c) microbial morphology.

3.3. Effect of Bulk pH on CaP Granules and Location of $Ca_x(PO_4)_y$ Precipitation. P enrichment along with the granule growth was only observed for the reactors fed with glucose (G1 and G2) but more pronounced for G1 (bulk pH 7.5) (Figure 3). The P content in fine particles (<0.4 mm diameter) was similar for both G1 and G2 (4.6 ± 1.3 and 4.6 ± 0.9 wt % P, respectively), while in particles of >1.4 mm diameter, it was significantly higher for G1 (8.7 ± 0.7 wt % P) than for G2 (and 5.4 ± 0.4 wt % P). For V1 and V2, the P content in particles of <0.4 mm diameter was 6.5 ± 1 wt % and even less with larger particle sizes, indicating that $Ca_x(PO_4)_y$ precipitation occurred mainly in the bulk as fines (Figure 3). The standard deviation was calculated for the average values of P content over time for each size fraction from each reactor. The two peaks in P content (per gram of dry matter) for V2 on day 89 for particles of <0.4 and 0.4−0.9 mm diameter might be related to accumulation of P precipitates at the bottom of the reactor in combination with low mixing.

For G1, the particle VSS content (or organic content) decreased along with granule size, from 73 wt % VSS for particles of <0.4 mm diameter to 36 wt % VSS for particles of >1.4 mm diameter (left panel of Figure 4). The VSS content in fine particles (<0.4 mm diameter) from G2 (49 wt % VSS) was lower than that from G1 as a result of the higher bulk pH, which likely enhanced bulk precipitation of $Ca_x(PO_4)_y$ and $CaCO_3$. This is supported by the relatively high Ca/P molar ratio in solids from G2, V1, and V2 (right panel of Figure 4) compared to hydroxyapatite (1.67), as demonstrated above by the molar ratio of accumulated Ca^{2+} and PO_4^{3-} in the same reactors. For G1, the average Ca/P molar ratio in solids (1.7 ± 0.2) matches with the molar ratio of accumulated Ca^{2+} and PO_4^{3-} and is close to the theoretical Ca/P molar ratio of hydroxyapatite (1.67). In the literature, the presence of CO_3^{2-} species is reported to have a detrimental effect on $Ca_x(PO_4)_y$ precipitation for solution pH between 7.5 and 11.[33,34] Moreover, bulk pH < 7.5 enables the development of the pH gradient between the edge and the granule center, which is crucial for preferred enrichment of $Ca_x(PO_4)_y$ within granules over its bulk precipitation, as shown in G1. The increase of bulk pH in G2 probably disrupted the pH gradient, decreasing the $Ca_x(PO_4)_y$ enrichment in the granules.

3.4. Comparison between CaP Granules Generated by Glucose (Bulk pH 7.5) and BW. In this study, CaP granulation was observed after 89 days while treating glucose with a simulated BW chemical matrix (cations and anions), using a UASB reactor (G1) under similar operating conditions as previously described for real BW.[6] The similarity between glucose (bulk pH 7.5) and BW CaP granules was evaluated according to the elemental composition and crystallographic aspects (Figure 5). CaP granulation was observed with real BW after similar operation time (100 days) as observed in this study.[2] After 200 days of operation, the concentration of CaP

DOI: 10.1021/acs.est.8b06230
Environ. Sci. Technol. 2019, 53, 1334−1343

granules (>0.4 mm diameter) at 5 cm from the bottom of G1 (glucose pH 7.5) was 51 ± 3 g of TSS L^{-1}_{sludge}, representing 88% of the total TSS concentration in the sludge bed (Figure 3). For BW as the influent (with Ca^{2+} addition), the concentration of CaP granules at the same reactor height was higher (75 ± 5 g of TSS L^{-1}_{sludge}) but the percentage was similar (90% of the total TSS concentration).[3] The presence of VSS (3.4 g L^{-1}) and suspended P (176 mg L^{-1}) in real BW, which were not included in the glucose and nutrient solutions fed to G1, are likely the reasons for the higher concentration of CaP granules using BW. The average P and Ca contents in CaP granules from G1 were 8.7 ± 0.7 and 18.2 ± 0.5 wt %, respectively (Ca/P molar ratio of 1.61 ± 0.17). BW CaP granules contained 6.7 ± 1.2 and 16.7 ± 2.8 wt % of P and Ca, respectively (Ca/P molar ratio of 1.93 ± 0.67).[3] The lower P content in BW CaP granules when compared to glucose granules can perhaps be explained by incorporation of non-biodegradable organic and inorganic substances from BW in the CaP granules. This is supported by the higher VSS content (47 ± 3 wt %) and higher Ca/P molar ratio (1.9) in BW granules than in glucose granules (40 ± 6 wt % and 1.6, respectively).[3] The magnesium content was below 2 wt % for both BW and glucose granules. The Pearson correlation factor between XRD spectra of BW and glucose granules was 0.9281 (n = 4210) and $r^2_{linear\ regression}$ of 0.86 (Figure 5). The dominant crystal phases in both glucose and BW CaP granules are hydroxyapatite and calcite, considering the reference XRD spectra in Figure 5. However, there is a significant percentage of amorphous material, which should be mostly amorphous calcium phosphate (ACP) with traces of amorphous calcium carbonate (ACC), according to ICP−OES results. This can be observed in both glucose and BW CaP granules. In BW CaP granules, the calculated amorphous content represents 76−90% of the mass weight, according to Rietveld pattern fitting.[4]

Cunha et al. proposed that internal hydrogenotrophic methanogenesis in the outer biofilm of CaP granules from BW promotes a pH gradient from 7.5 at the edge to 8 in the granule core, which is essential for preferable $Ca_x(PO_4)_y$ formation in the granules over bulk precipitation.[4] In this study, we confirmed that CaP granulation is biologically induced. The biological role is based on the production of extracellular biopolymers, which are used for biofilm formation, trapping microorganisms, and $Ca_x(PO_4)_y$ particles. The produced biopolymers and Ca^{2+} complexation act as gluing agents, strengthening the organic−inorganic matrix.[35] Then, local microbial syntrophy (H_2 producers and consumers) promote the development of the increasing pH gradient between the bulk and the granule center as previously reported by Cunha et al., which is essential for $Ca_x(PO_4)_y$ enrichment in the granules.[4] The COD used for biomass growth in G1 represented 11% (0.08 g of VSS g^{-1} of $COD_{influent}$) of the total incoming COD, while the COD used for biomass growth in V1 represented only 4% (0.03 g of VSS g^{-1} of $COD_{influent}$). Inhibition by pH was not observed for G1 or V1. Also, at 25 °C, the biomass yield for anaerobic treatment of BW (0.09 g of VSS g^{-1} of $COD_{influent}$) was closer to G1 than to V1. The higher biomass yield obtained by acidogenesis (fermentation) when compared to only acetogenesis and methanogenesis might be a stimulator for CaP granulation. Thus, for the implementation of the CaP granulation process in other wastewater types, particular attention should be given to the carbon source composition besides the chemical matrix (cations and anions) and the thermodynamic conditions (bulk pH) for $Ca_x(PO_4)_y$ precipitation.

3.5. Strategy for Collection of Granules and Stimulation of Granule Formation and Growth. A strategy for collection of P-rich granules of a certain size in a methane-producing bioreactor can be derived from the results and insights provided by this study. It was shown that the carbon source, which influences the production of EPS, and bulk solution pH are key factors to produce CaP granules with adequate size for collection and to ensure P enrichment in the granules over $Ca_x(PO_4)_y$ precipitation in the bulk as fines. The bulk pH was measured daily, but as a result of the manual control (twice a week), the standard deviation was high, especially for G2 (0.39 units). Nevertheless, G2 ran with bulk pH above 7.8 for 82% of the experimental time and for 60% with bulk pH between 7.8 and 8.2. Bulk pH above 7.8 triggers unwanted precipitation of fines in the bulk of the reactor, as shown by the higher concentration of particles of <0.4 mm diameter in G2 than in G1 (Figure 2). These fines are hard to separate from dispersed biomass, and thus, they reduce the efficiency of $Ca_x(PO_4)_y$ collection from biomass (BW sludge). The high bulk pH of G2 also results in a 38% lower P content for CaP granules of >0.4 mm diameter (Figure 3) when compared to G1. Thus, to prevent precipitation of $Ca_x(PO_4)_y$ fines in the bulk solution and to promote P enrichment in the granules for growth of the $Ca_x(PO_4)_y$ core, the bulk pH should be controlled.

The outer biofilm (VSS) of CaP granules (>0.4 mm diameter) from G2 represents about 32−51% of the weight, but it is essential during the growth stage to sustain the $Ca_x(PO_4)_y$ core development. A new reactor design was previously proposed by Cunha et al., where internal gas mixing facilitates the accumulation of mature CaP granules at the bottom of the UASB reactor while promoting the formation and growth of new granules in the upper part of the sludge bed.[4] The applied shear by the internal mixing is expected to reduce the biofilm thickness (VSS content) in mature CaP granules before collection from the bottom of the reactor. The loss of biomass within the residual biofilm on CaP granules will hardly affect the treatment performance as previously observed by Cunha et al.[3] This is supported by the long solids retention time (SRT) obtained in a UASB reactor treating BW and containing CaP granules, which ranges from 163 to 239 days.[3] A post-separation, for instance, by size exclusion and pressured water spraying, would further reduce the organic content and increase the mass percentage of P in the recovered granules.

Simultaneous recovery of P and CH_4 in a single bioreactor shortens the treatment scheme for vacuum-collected BW, by avoiding a subsequent reactor for P recovery. The capital expenditures (CAPEX) for treatment of source-separated BW are directly reduced, with decentralized sanitation simplified. Moreover, 40−60% of P in BW is accumulated in the UASB reactor, even without Ca^{2+} addition.[2,36] Consequently, recovery of P from the effluent of the UASB reactor will have a limited yield. The implementation of a CaP granulation process with Ca^{2+} addition can increase the accumulation of P in the UASB reactor to 90%, mostly as CaP granules (>0.4 mm diameter), which can be harvested. Additionally, as demonstrated in this study, the formation of CaP granules with 8.7 wt % P and accumulation in the UASB reactor of 88% of P occur even with 70% lower total P concentration in the influent stream, when compared to BW. Thus, this recovery process

DOI: 10.1021/acs.est.8b06230
Environ. Sci. Technol. 2019, 53, 1334−1343

could be used for other wastewater streams with a lower P concentration.

■ ASSOCIATED CONTENT

Supporting Information

The Supporting Information is available free of charge on the ACS Publications website at DOI: 10.1021/acs.est.8b06230.

Additional XRD spectra of the inoculum, G1, G2, V1, and V2 presented as figures S1.1, S1.2, S1.3, S1.4, and S1.5, respectively (subsection S1), bulk pH, CH_4 production, and PO_4^{3-} and Ca^{2+} removals during the operation period presented as Figures S2.1a, S2.1b, and S2.2, respectively, and Table S2.1 presenting the dosed amount of NaOH and the resulting concentration of Na^+ in each influent stream (subsection S2), and concentration of loose and bound extracellular biopolymers for each reactor presented as Figure S3.1 (subsection S3) (PDF)

■ AUTHOR INFORMATION

Corresponding Author

*Telephone: +31-317-483-851. E-mail: renata.vanderweijden@wur.nl.

ORCID

Jorge Ricardo Cunha: 0000-0002-6791-0119

Notes

The authors declare no competing financial interest.

■ ACKNOWLEDGMENTS

The authors thank Joana Carvalho and Mbuotidem Ikono for their contribution in the experimental work. This work was performed in the cooperation framework of Wetsus, European Centre of Excellence for Sustainable Water Technology (www.wetsus.eu). Wetsus is co-funded by the Dutch Ministry of Economic Affairs and Ministry of Infrastructure and Environment, the Province of Fryslân, and the Northern Netherlands Provinces. The authors thank the members of the research theme Source Separated Sanitation and University of Groningen/Campus Fryslân for the shared knowledge and support.

■ REFERENCES

(1) Tervahauta, T.; van der Weijden, R. D.; Flemming, R. L.; Hernández Leal, L.; Zeeman, G.; Buisman, C. J. N. Calcium phosphate granulation in anaerobic treatment of black water: A new approach to phosphorus recovery. *Water Res.* **2014**, *48*, 632−642.

(2) Cunha, J. R.; Tervahauta, T.; van der Weijden, R. D.; Hernández Leal, L.; Zeeman, G.; Buisman, C. J. N. Simultaneous recovery of calcium phosphate granules and methane in anaerobic treatment of black water: Effect of bicarbonate and calcium fluctuations. *J. Environ. Manage.* **2018**, *216*, 399−405.

(3) Cunha, J. R.; Schott, C.; van der Weijden, R. D.; Leal, L. H.; Zeeman, G.; Buisman, C. Calcium addition to increase the production of phosphate granules in anaerobic treatment of black water. *Water Res.* **2018**, *130*, 333−342.

(4) Cunha, J. R.; Tervahauta, T.; Van Der Weijden, R. D.; Temmink, H.; Hernández Leal, L.; Zeeman, G.; Buisman, C. J. N. The Effect of Bioinduced Increased pH on the Enrichment of Calcium Phosphate in Granules during Anaerobic Treatment of Black Water. *Environ. Sci. Technol.* **2018**, *52* (22), 13144−13154.

(5) Batstone, D. J.; Keller, J.; Blackall, L. L. The influence of substrate kinetics on the microbial community structure in granular anaerobic biomass. *Water Res.* **2004**, *38* (6), 1390−1404.

(6) De Graaff, M. S.; Temmink, H.; Zeeman, G.; Buisman, C. J. N. Anaerobic Treatment of Concentrated Black Water in a UASB Reactor at a Short HRT. *Water* **2010**, *2* (1), 101−119.

(7) Kujawa-Roeleveld, K.; Zeeman, G. Anaerobic treatment in decentralised and source-separation-based sanitation concepts. *Rev. Environ. Sci. Bio/Technol.* **2006**, *5* (1), 115−139.

(8) Tchobanoglous, G.; Burton, F. L.; Stensel, H. D. *Wastewater Engineering: Treatment and Reuse*, 4th ed.; McGraw-Hill: New York, 2004.

(9) Liu, Y.-Q.; Liu, Y.; Tay, J.-H. The effects of extracellular polymeric substances on the formation and stability of biogranules. *Appl. Microbiol. Biotechnol.* **2004**, *65* (2), 143−148.

(10) Stams, A. Metabolic Interactions Between Anaerobic-Bacteria in Methanogenic Environments. *Antonie van Leeuwenhoek* **1994**, *66* (1−3), 271−294.

(11) Schmidt, J. E.; Ahring, B. K. Extracellular polymers in granular sludge from different upflow anaerobic sludge blanket (UASB) reactors. *Appl. Microbiol. Biotechnol.* **1994**, *42* (2−3), 457−462.

(12) Zhou, W.; Imai, T.; Ukita, M.; Sekine, M.; Higuchi, T. Triggering forces for anaerobic granulation in UASB reactors. *Process Biochem.* **2006**, *41* (1), 36−43.

(13) de Graaf, R.; van Hell, A. J. *Nieuwe Sanitatie Noorderhoek, Sneek: Deelonderzoeken. Rapport 48*; Stichting Toegepast Onderzoek Waterbeheer (STOWA): Amersfoort, Netherlands, 2014.

(14) Angelidaki, I.; Alves, M.; Bolzonella, D.; Borzacconi, L.; Campos, L.; Guwy, A.; Jenicek, P.; Kalyuzhnyi, S. V.; van Lier, J. B. *Anaerobic Biodegradation, Activity and Inhibition (ABAI) Task Group Meeting 9th to 10th October 2006, in Prague*; Institute of Environment & Resources, Technical University of Denmark: Kongens Lyngby, Denmark, 2007.

(15) Seckler, M. M.; Bruinsma, O. S. L.; Van Rosmalen, G. M. Calcium phosphate precipitation in a fluidized bed in relation to process conditions: A black box approach. *Water Res.* **1996**, *30* (7), 1677−1685.

(16) Clesceri, L. S.; Rica, E. W.; Baird, R. B.; Eaton, A. D. *Standard Methods for the Examination of Water and Wastewater*, 20th ed.; American Public Health Association (APHA), American Water Works Association (AWWA), and Water Environment Federation (WEF): Washington D.C., 1998.

(17) Ismail, S. B.; de La Parra, C. J.; Temmink, H.; van Lier, J. B. Extracellular polymeric substances (EPS) in upflow anaerobic sludge blanket (UASB) reactors operated under high salinity conditions. *Water Res.* **2010**, *44* (6), 1909−1917.

(18) Frølund, B.; Palmgren, R.; Keiding, K.; Nielsen, P. H. Extraction of extracellular polymers from activated sludge using a cation exchange resin. *Water Res.* **1996**, *30* (8), 1749−1758.

(19) Duarte, A. C.; Anderson, G. K. Inhibition modelling in anaerobic digestion. *Water Sci. Technol.* **1982**, *14* (6−7), 749−763.

(20) Fukuzaki, S.; Nishio, N.; Nagai, S. Kinetics of the methanogenic fermentation of acetate. *Appl. Environ. Microbiol.* **1990**, *56* (10), 3158−3163.

(21) Fang, H. H. P.; Liu, H. Effect of pH on hydrogen production from glucose by a mixed culture. *Bioresour. Technol.* **2002**, *82* (1), 87−93.

(22) Zoetemeyer, R. J.; van den Heuvel, J. C.; Cohen, A. pH influence on acidogenic dissimilation of glucose in an anaerobic digestor. *Water Res.* **1982**, *16* (3), 303−311.

(23) Boone, D. R.; Xun, L. Effects of pH, Temperature, and Nutrients on Propionate Degradation by a Methanogenic Enrichment Culture. *Appl. Environ. Microbiol.* **1987**, *53* (7), 1589−1592.

(24) Ganidi, N.; Tyrrel, S.; Cartmell, E. Anaerobic digestion foaming causes—A review. *Bioresour. Technol.* **2009**, *100* (23), 5546−5554.

(25) Habraken, W. J. E. M.; Tao, J. H.; Brylka, L. J.; Friedrich, H.; Bertinetti, L.; Schenk, A. S.; Verch, A.; Dmitrovic, V.; Bomans, P. H. H.; Frederik, P. M.; Laven, J.; van der Schoot, P.; Aichmayer, B.; de With, G.; DeYoreo, J. J.; Sommerdijk, N. A. J. M. Ion-association complexes unite classical and non-classical theories for the biomimetic nucleation of calcium phosphate. *Nat. Commun.* **2013**, *4*, 1507.

(26) Li, X. Y.; Yang, S. F. Influence of loosely bound extracellular polymeric substances (EPS) on the flocculation, sedimentation and dewaterability of activated sludge. *Water Res.* **2007**, *41* (5), 1022−1030.
(27) van Lier, J. B.; Mahmoud, N.; Zeeman, G. Anaerobic Wastewater Treatment. In *Biological Wastewater Treatment: Principles, Modelling and Design*; Henze, M., van Loosdrecht, M. C. M., Ekama, G. A., Brdjanovic, D., Eds.; IWA Publishing: London, U.K., 2008; pp 401−442.
(28) Liu, X. M.; Sheng, G. P.; Luo, H. W.; Zhang, F.; Yuan, S. J.; Xu, J.; Zeng, R. J.; Wu, J. G.; Yu, H. Q. Contribution of extracellular polymeric substances (EPS) to the sludge aggregation. *Environ. Sci. Technol.* **2010**, *44* (11), 4355−4360.
(29) Ding, Z.; Bourven, I.; Guibaud, G.; van Hullebusch, E. D.; Panico, A.; Pirozzi, F.; Esposito, G. Role of extracellular polymeric substances (EPS) production in bioaggregation: Application to wastewater treatment. *Appl. Microbiol. Biotechnol.* **2015**, *99* (23), 9883−9905.
(30) Hulshoff Pol, L. W.; de Castro Lopes, S. I.; Lettinga, G.; Lens, P. N. L. Anaerobic sludge granulation. *Water Res.* **2004**, *38* (6), 1376−1389.
(31) Liu, Y.; Tay, J.-H. State of the art of biogranulation technology for wastewater treatment. *Biotechnol. Adv.* **2004**, *22* (7), 533−563.
(32) Liu, Y.; Xu, H. L.; Show, K. Y.; Tay, J.-H. Anaerobic granulation technology for wastewater treatment. *World J. Microbiol. Biotechnol.* **2002**, *18* (2), 99−113.
(33) Cao, X.; Harris, W. Carbonate and magnesium interactive effect on calcium phosphate precipitation. *Environ. Sci. Technol.* **2008**, *42* (2), 436−442.
(34) Ferguson, J. F.; McCarty, P. L. Effects of Carbonate and Magnesium on Calcium Phosphate Precipitation. *Environ. Sci. Technol.* **1971**, *5* (6), 534−540.
(35) More, T. T.; Yadav, J. S. S.; Yan, S.; Tyagi, R. D.; Surampalli, R. Y. Extracellular polymeric substances of bacteria and their potential environmental applications. *J. Environ. Manage.* **2014**, *144*, 1−25.
(36) de Graaff, M. S.; Temmink, H.; Zeeman, G.; Buisman, C. J. N. Energy and phosphorus recovery from black water. *Water Sci. Technol.* **2011**, *63* (11), 2759−2765.

DOI: 10.1021/acs.est.8b06230
Environ. Sci. Technol. 2019, 53, 1334−1343